Available online at www.sciencedirect.com
SCIENCE DIRECT
Biochimica et Biophysica Acta 1761 (2006) 324–334
BIOCHIMICA ET BIOPHYSICA ACTA
BBA
http://www.elsevier.com/locate/bba

Plant fatty acid (ethanol) amide hydrolases

Rhidaya Shrestha [a,1], Sang-chul Kim [a], John M. Dyer [b], Richard A. Dixon [c], Kent D. Chapman [a,*]

[a] *University of North Texas, Center for Plant Lipid Research, Department of Biological Sciences, Denton, P.O. Box 305220, TX 76203, USA*
[b] *USDA-ARS Southern Regional Research Center, New Orleans, LA 70124, USA*
[c] *Samuel Roberts Noble Foundation, Plant Biology Division, Ardmore, OK 73402, USA*

Received 6 October 2005; received in revised form 6 March 2006; accepted 7 March 2006
Available online 31 March 2006

Abstract

Fatty acid amide hydrolase (FAAH) plays a central role in modulating endogenous *N*-acylethanolamine (NAE) levels in vertebrates, and, in part, constitutes an "endocannabinoid" signaling pathway that regulates diverse physiological and behavioral processes in animals. Recently, an *Arabidopsis* FAAH homologue was identified which catalyzed the hydrolysis of NAEs in vitro suggesting a FAAH-mediated pathway exists in plants for the metabolism of endogenous NAEs. Here, we provide evidence to support this concept by identifying candidate FAAH genes in monocots (*Oryza sativa*) and legumes (*Medicago truncatula*), which have similar, but not identical, exon–intron organizations. Corresponding *M. truncatula* and rice cDNAs were isolated and cloned into prokaryotic expression vectors and expressed as recombinant proteins in *Escherichia coli*. NAE amidohydrolase assays confirmed that these proteins indeed catalyzed the hydrolysis of ^{14}C-labeled NAEs in vitro. Kinetic parameters and inhibition properties of the rice FAAH were similar to those of *Arabidopsis* and rat FAAH, but not identical. Sequence alignments and motif analysis of plant FAAH enzymes revealed a conserved domain organization for these members of the amidase superfamily. Five amino-acid residues determined to be important for catalysis by rat FAAH were absolutely conserved within the FAAH sequences of six plant species. Homology modeling of the plant FAAH proteins using the rat FAAH crystal structure as a template revealed a conserved protein core that formed the active site of each enzyme. Collectively, these results indicate that plant and mammalian FAAH proteins have similar structure/activity relationships despite limited overall sequence identity. Defining the molecular properties of NAE amidohydrolase enzymes in plants will help to better understand the metabolic regulation of NAE lipid mediators.

Keywords: Lipid metabolism; N-acylethanolamines; Fatty acid amide hydrolase

1. Introduction

N-Acylethanolamines (NAEs)[3] are fatty acid amide derivatives comprising fatty acids of various chain lengths linked to the amino group of ethanolamine. They are endogenous lipid constituents in both animal and plant systems that occur in relatively trace concentrations. Several NAE types in mammals are generally accepted as endogenous lipid mediators that regulate a wide range of physiological processes, including neurotransmission [1], embryo development and implantation [2], immune responses [3], and cell proliferation [4], often (but not always) through their interaction with membrane bound cannabinoid (CB) receptors [5]. A fatty acid amide hydrolase (FAAH) is believed to terminate the regulatory cascade triggered by NAEs in these diverse processes by hydrolyzing the molecules into corresponding free fatty acids and ethanolamine [6]. Thus, FAAH-modulation of NAE levels has become an important focus for understanding the mechanistic action of the "endocannabinoid" signaling system in vertebrates [7], and a convenient target for the development of novel therapeutics [8].

NAEs in plants, like animals, have potent biological activities at reasonably low concentrations (reviewed recently in [9]). For example, sub-micromolar to low micromolar

Abbreviations: bp, base pairs; FAAH, fatty acid amide hydrolase; FFA, free fatty acid; MAFP, methyl archidonyl fluorophosphonate; NAE, N-acylethanolamine; numerical designation of acyl chain is number of carbon atoms, number of double bonds; ORF, open reading frame; URB597, 3′-carbamoyl-biphenyl-3-yl-cyclohexylcarbamate; UTR, untranslated region

* Corresponding author. Tel.: +1 940 565 2969; fax: +1 940 369 8656.
E-mail address: chapman@unt.edu (K.D. Chapman).
[1] Current address: Michigan State University—Department of Energy, Plant Research Laboratory, East Lansing, MI 48824, USA.

1388-1981/$ - see front matter © 2006 Elsevier B.V. All rights reserved.
doi:10.1016/j.bbalip.2006.03.004

concentrations of NAE14:0 activated defense gene expression in cell suspensions and leaves of tobacco plants [10], marked by an increase in phenylalanine-lyase (*PAL2*) transcript abundance. The activation of *PAL2* expression was specific for acylethanolamides (since free fatty acids showed no effect), and was blocked by antagonists of mammalian CB receptors [11]. In other work, *Arabidopsis* seedlings germinated in and maintained on micromolar concentrations of NAE12:0 showed marked developmental abnormalities in young roots, that again were selective for acylethanolamides, and in this case were restricted to the short/medium chain NAEs [12]. While these pharmacological approaches show that the application of NAEs to plants can elicit profound physiological and cellular changes, additional experimental evidence is needed to link the endogenous metabolism of these bioactive lipids to their physiological functions.

In plants, NAEs occur in a number of tissues and their levels have been reported to change in response to biotic stress and changes in development [9]. For example, NAEs were present at ppm levels in desiccated seeds and then dropped to barely detectable levels coincident with seed imbibition and germination [13]. The metabolism of NAEs was traced in vivo in imbibed seeds, and reconstituted in vitro in microsomes of imbibed seeds, and shown to involve, in part, the hydrolysis to free fatty acids and ethanolamine, presumably by a FAAH-like enzyme activity [14]. Bioinformatics approaches and heterologous protein expression led to the molecular identification of an amidohydrolase from *Arabidopsis thaliana* that hydrolyzed a wide range of acylethanolamides, including those present in desiccated seeds [15]. Consequently, we proposed that plants, like animals, possess the capability to regulate endogenous NAE levels by a FAAH-like enzyme.

Here, we expand the knowledge-base of lipid metabolism by providing molecular and biochemical support for existence of FAAH genes and enzymes in diverse plant species. Genes in rice and *Medicago truncatula* were identified and compared to the FAAH gene in *Arabidopsis thaliana* (At5g64440), and found to have similar, albeit complex, exon/intron organizations. Coding sequences from these plant species were isolated and functionally expressed in *E. coli*, and, consistent with the *Arabidopsis* and rat FAAH proteins, the recombinant rice and *M. truncatula* enzymes indeed hydrolyzed NAEs. Overall, these results help to functionally define the group of enzymes that metabolize NAEs in plants, information critical for understanding the regulation of endogenous NAE signaling pathways in higher plant systems.

2. Results

The *Arabidopsis* FAAH gene (At5g64440) sequence was used to query other plant genome databases for candidate FAAH orthologs. FAAH orthologous genes were identified in *Medicago truncatula* and *Oryza sativa* (Fig. 1). Although the number of predicted exons differed, the overall structural organization of candidate FAAH genes identified in *M. truncatula* and rice was similar to that of *Arabidopsis* FAAH (Fig. 1). The coding sequence of the *M. truncatula* gene encompassed 10,376 bp and is located on chromosome 2 (Accession AC148396). The *M. truncatula* FAAH gene had 20 exons including 5′ and 3′ UTR (Fig. 1A). The coding sequence of the rice gene was located on chromosome 4 and spanned 9593 bp, and had 19 exons including 5′ and 3′ UTR (Fig. 1B sequence from BAC clone: OSJNBa0068L06; Accession AL606442). These were compared to the shorter *Arabidopsis*

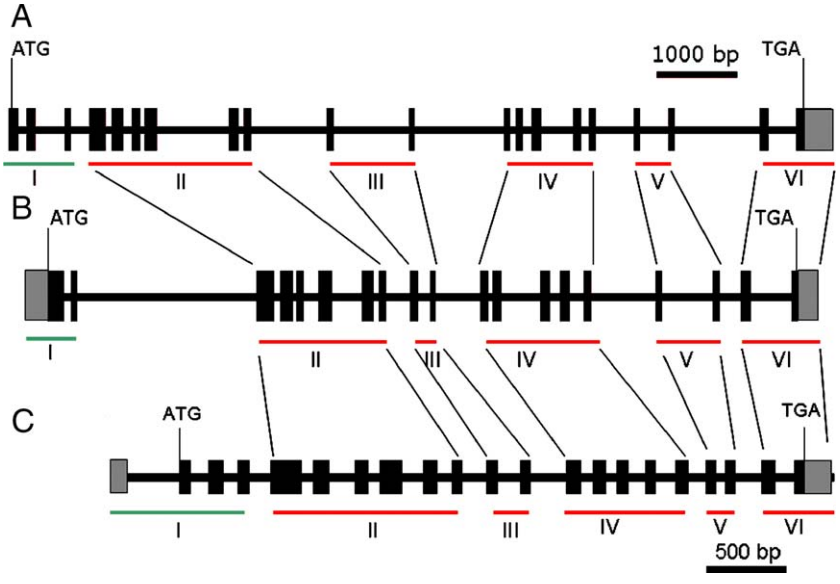

Fig. 1. Schematic comparison of the exon organization of the *FAAH* genes identified in *Medicago truncatula* (A), rice (B), and *Arabidopsis* (C). Exons are depicted as vertical bars; those that are part of the ORF are black whereas those that encode UTR are gray. The scale for A and B is at the top of the diagram, and the scale for the shorter *Arabidopsis* gene (At5g64440) is at the bottom of the diagram. Exons were divided into six groups designated with Roman numerals. Organization within group I is variable and is underlined in green. Organization of groups II through VI are highly conserved and are underlined in red. ATG at the 5′ ends and TGA at the 3′ ends define the ORF for each gene. Exons in groups II and III encode the amidase signature sequence (see Fig. 9). (For interpretation of the references to colour in this figure legend, the reader is referred to the web version of this article.)

gene of 4,689 bp which had 20 exons including 5′ and 3′ UTR ([15]; Fig. 1C). Gene models for *M. truncatula* and rice genes were compared to our isolated cDNA sequences (Supplementary Figs. S1 and S2), and a rice tentative consensus (TC) sequence at www.tigr.org (Table 1), to verify exon/intron annotation. The three orthologous plant FAAH genes were divided into 6 groups of exons (Fig. 1). The organization of five of the six groups was highly conserved among these diverse plant species. The number of exons (and their organization) in the designated group I differed among the three genes, corresponding to the 5′UTR and the 5′ end of the open reading frame (ORF) of the coding sequences.

To assess if the *M. truncatula* and rice genes encoded functional FAAH enzymes, corresponding cDNAs were first isolated and sequenced (Supplementary Figs. S1 and S2). Identification of the *M. truncatula* cDNA sequence relied on the characterization of an expressed sequence tag (EST) cDNA that was from an elicited cell suspension cDNA library (Accession AW695697). The EST sequence deposited in GenBank overlapped with the 5′UTR and 5′ end of the ORF of the *M. truncatula* gene (italicized sequence in Fig. S1). The nucleotide sequence of this cDNA was determined completely on both strands and found to encode a full-length sequence of 2,336 bp (Fig. S1). The deduced amino acid sequence was 607 amino acids in length with a predicted molecular mass of 66,207 and a pI of 5.83, properties similar to the *Arabidopsis* FAAH [15].

To identify a rice cDNA, oligonucleotide primers were designed to the 5′ and 3′ ends of the predicted ORF (from the gene sequence), and a cDNA fragment was amplified from total seedling RNA by reverse-transcriptase (RT) PCR. The DNA fragment was cloned directly into pTrcHis2 expression plasmid (Invitrogen) for in-frame protein expression and sequenced completely on both strands for confirmation (Fig. S2). The predicted protein product is 601 amino acids in length, has a predicted molecular mass of 65,809 and a predicted pI of 6.00, all properties that were similar to those of *M. truncatula* FAAH (Fig. S1) and the *Arabidopsis* recombinant FAAH [15]. A coded segment identified in the cDNA, highlighted in bold, was not in the ORF from some earlier gene model predictions (Accession AL606442). Together, these cDNA sequences isolated from both *M. truncatula* and rice helped to annotate correctly the corresponding genes and verified their expression.

Table 1
Tentative consensus (TC, as of 10/15/04) identifiers of the orthologous group of plant sequences that includes the rice and *Medicago truncatula* FAAH sequences in this manuscript

Plant	TC identifier	% identity Arab FAAH	*P* value	Length
Arabidopsis	TC210025	100	0.00	2145
Barley	TC111212	65	2.6e–91	1217
Cotton	TC21641	71	1.1e–67	717
Grape	TC36243	73	1.0e–143	1301
Maize	TC230081	66	8.8e–26	377
Potato	TC76474	64	2.0e–62	918
Rice	TC188324	64	3.2e–132	1820
Sugarcane	TC18099	65	1.4e–42	624
Sorghum	TC87636	67	8.7e–30	439
Soybean	TC179281	71	4.6e–51	552
Soybean	TC199488	72	9.6e–53	554
Tomato	TC117552	69	3.5e–75	859
Tomato	TC132131	68	1.4e–166	1839
Wheat	TC150217	64	3.6e–116	1589
M. truncatula	AW695697 (single)	71	4.0e–93	963

Assembled by The Institute for Genomic Resources (www.tigr.org) as tentative ortholog group 520300 (as of 10/15/04), except for *Medicago truncatula* which not assembled into a TC (AW695697 is a singleton). TCs built with available DNA sequences in various DNA databases including EST and other partial nucleotide sequences.
% identity is at the nucleotide level and the match length is provided over which the *P* value was calculated.

A list of plant FAAH sequences is summarized and compared in Table 1 including the *Arabidopsis* FAAH [15], the *M. truncatula* (Fig. S1) and rice (Fig. S2) sequences. The TC identifiers are from the assembled orthologous group at www.tigr.org. Predicted full-length sequences are now represented in databases from four diverse plant species, *Arabidopsis*, *M. truncatula*, rice and tomato, ranging in nucleotide sequence identity from 64% to 71%. Additionally, predicted partial length sequences are represented from soy, tomato, sorghum, wheat, potato, maize, grape, cotton and barley. Two plants, soy and tomato, may express more than one FAAH mRNA, but this remains to be evaluated by obtaining full-length sequences and performing functional expression studies. There were no paralogous sequences identified in the rice or *Medicago* genomes, however.

To assess if the identified FAAH cDNAs encoded functional NAE amidohydrolases, the ORFs of both *M. truncatula* FAAH and rice FAAH were cloned into the prokaryotic expression vector pTrcHis2 (Invitrogen) for in-frame recombinant protein expression in *E. coli*. Lysates of *E. coli* cells (Top10, Invitrogen), induced to express the recombinant FAAH proteins, were screened for their ability to catalyze the conversion of [^{14}C] NAEs to [^{14}C] free fatty acids. A similar strategy was employed successfully to demonstrate functional rat [16] and *Arabidopsis* [15] recombinant enzymes. Representative radiochromatograms of assay reaction mixture lipids are shown in Fig. 2. Positive controls, cells expressing rat (Rat FAAH) or *Arabidopsis* (At NAE AHase) NAE amidohydrolases, are shown in panels A and F, respectively, marking the position of both substrate (in this case [^{14}C]-NAE 18:2) and product ([^{14}C]-FFA 18:2). Cells expressing the *M. truncatula* FAAH (Mt NAE AHase) in the forward orientation with respect to the *lacZ* promoter (panel B) catalyzed hydrolysis of NAE, whereas cells harboring the FAAH in the reverse orientation (panel C), did not. The same results were obtained with *E. coli* cells expressing the rice FAAH (Os NAE AHase) in the forward or reverse orientations (panels D and E, respectively). Results with the cells harboring plasmids with the prospective plant FAAH cDNAs in reverse orientation (panels C and E), indicated that *E. coli* cells had no appreciable endogenous capability to hydrolyze NAEs. Hence the recovery of NAE amidohydrolase activity in cells expressing recombinant plant FAAHs (panels B, D, and F) is a clear indication that these cDNAs encode functional FAAH enzymes.

The biochemical properties of the recombinant rice FAAH were compared to those of the *Arabidopsis* FAAH in terms of

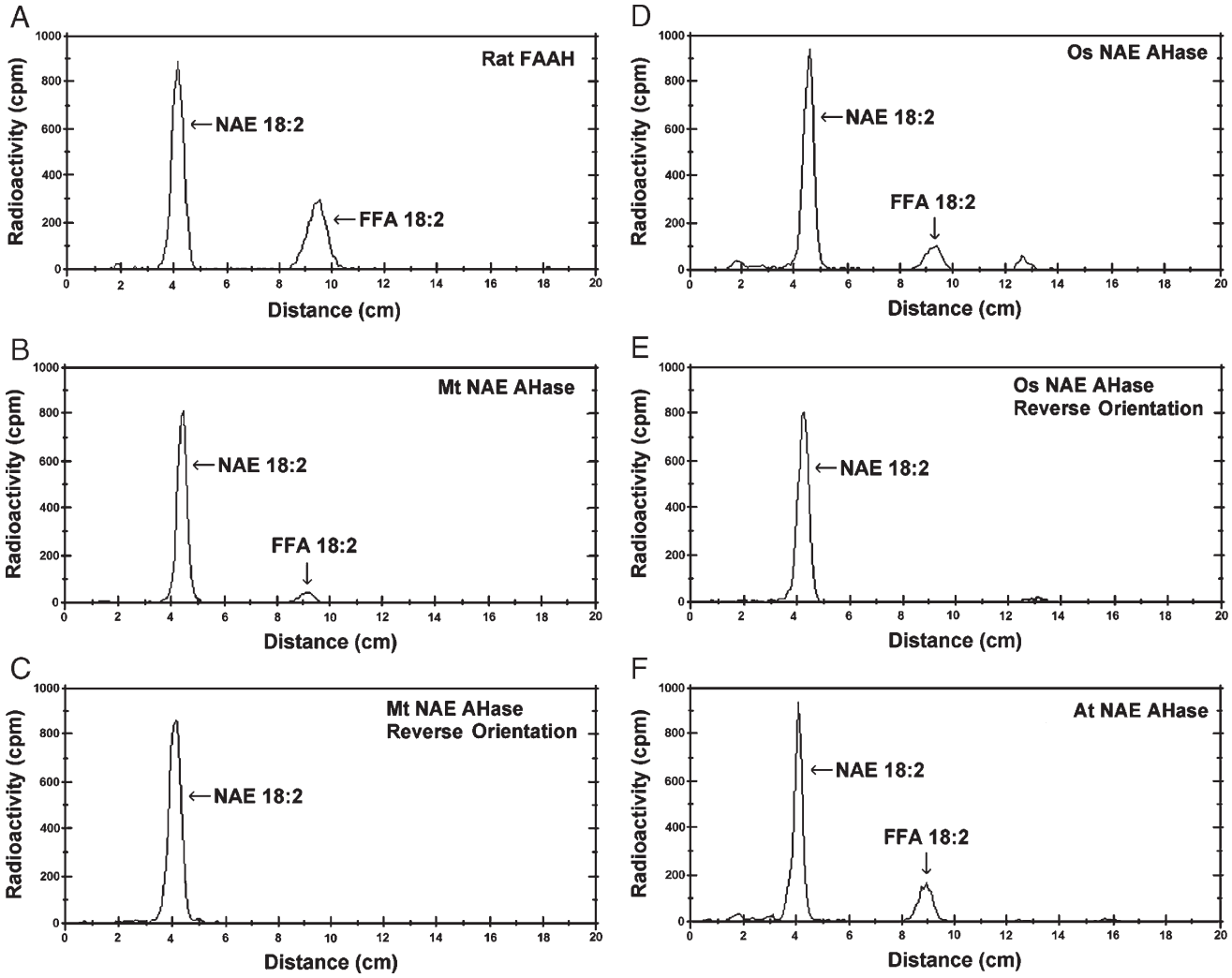

Fig. 2. Representative radiochromatograms of lipids extracted from reaction mixtures following assays of NAE amidohydrolase (NAE AHase) activity (measured as formation of radiolabeled FFA 18:2 from radiolabeled NAE18:2 in this case) and separated by Silica gel-thin layer chromatography (TLC). In all cases, *E. coli* lysate (2 μg protein for rat and *Arabidopsis*; 20 μg protein for rice and *Medicago*) was used as the enzyme source, from cells harboring the following different cDNAs in pTrcHis2 expression plasmids: A) rat FAAH cDNA, B) Mt cDNA forward orientation, C) Mt cDNA cloned in reverse orientation so as not to direct expression of a recombinant protein, D) Os cDNA forward orientation, E) Os cDNA cloned in reverse orientation so as not to direct expression of a recombinant protein, F) At FAAH cDNA.

kinetic parameters (Figs. 3 and 4), inhibition by rat FAAH inhibitors, MAFP and URB597 (Fig. 5), and abundance of full-length proteins in *E. coli* lysates (Fig. 6). The rice FAAH, like the *Arabidopsis* (and rat) FAAH, hydrolyzed a wide range of NAE types including NAE12:0, NAE16:0 and NAE18:2 in a concentration dependent manner (Fig. 3). The rice FAAH, like the *Arabidopsis* FAAH, exhibited typical Michaelis–Menten behavior toward all NAE substrates (Fig. 3) and displayed a pH dependence such that enzyme behavior, judged as V_{max}/K_m, was optimal at pH 9 for essentially all NAE substrates (Fig. 4). Direct comparisons of apparent V_{max} cannot be made here between the rice and *Arabidopsis* enzymes, since these initial velocity measurements were made with enzymes in crude lysates. Measuring enzyme activity in lysates was necessary due to poor stability of the rice enzyme to the purification procedures. This instability is readily apparent as differences in protein levels and degradation products between the different plant recombinant FAAH proteins in *E. coli* (Fig. 6), and helps to account for absolute differences in apparent V_{max} between *Arabidopsis* and rice FAAH. Nonetheless, some inferences can be made about substrate preferences of these enzymes by taking into account the apparent V_{max}/K_m of the enzymes toward the different NAE types. The rice FAAH appeared to utilize NAE18:2 most efficiently, whereas *Arabidopsis* FAAH appeared to utilize all NAE types with similar efficiency.

As expected the rice FAAH activity, like the *Arabidopsis* FAAH, was inhibited by MAFP in a concentration-dependent manner (Fig. 4). MAFP binds to rat FAAH irreversibly and has been crystallized in the acyl domain of the active site [17,18]. The potent inhibition of rice FAAH by MAFP and the similar kinetic properties between rice and *Arabidopsis* FAAH suggests that indeed the rice enzyme is a functional FAAH homologue. Interestingly, neither the *Arabidopsis* nor the rice

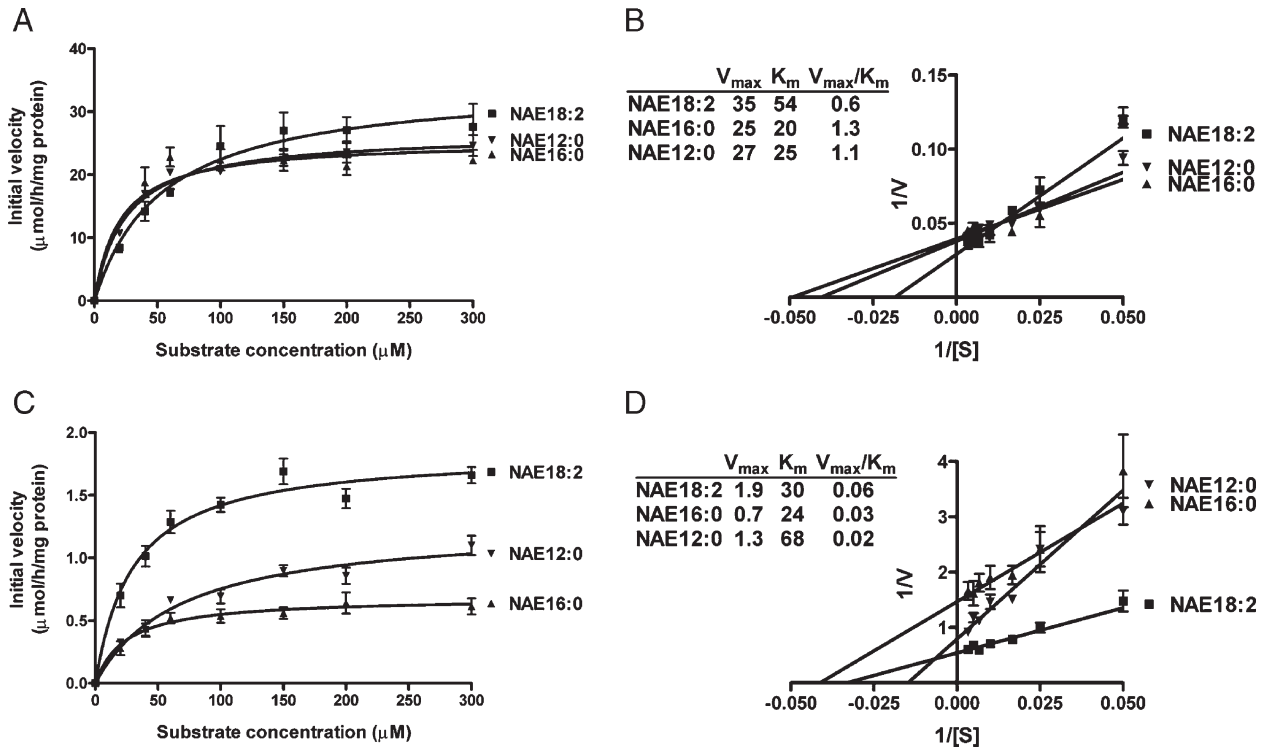

Fig. 3. Kinetic characterization of *A. thaliana* and rice NAE amidohydrolases. Initial velocities were measured at increasing concentrations of respective [1-^{14}C]NAE. Reactions were initiated by the addition of *E. coli* cell lysates expressing *A. thaliana* (A, B) or rice (C, D) NAE amidohydrolases (2 μg for *A. thaliana*, 20 μg for rice) and were carried out in 50 mM Bis–Tris buffer (pH 9.0) in a final volume of 0.4 mL. Data points in A and B represent means ± S.D. of triplicate assays. Plots were generated with Prism software version 3.0 (GraphPad Software, San Diego).

FAAH was inhibited by URB597 (Fig. 4), another specific inhibitor of rat FAAH that covalently modifies S241 in the active site. Notably, this serine residue is conserved among rat and plant FAAH protein sequences. The URB597 inhibitor is believed to gain access to the rat FAAH catalytic site via the cytoplasmic access channel [18], which suggests that there are some structural differences between the vertebrate and plant FAAH enzymes within this region of the FAAH protein. A structural difference is certainly supported by the low level of identity between rat and *Arabidopsis* FAAH ***outside*** the amidase signature domain (less than 20% identity [15]). By way of comparison, the URB597 was a potent inhibitor of the rat FAAH enzyme activity in our hands with 2 nM reducing activity by 50% and 100 nM essentially eliminating enzymatic activity (data not shown). The differential inhibition of plant FAAH activity by two well-characterized inhibitors of mammalian FAAH [18] could provide an important diagnostic tool in future detailed comparisons between the structure/activity relationships of the mammalian and plant FAAH enzymes.

An alignment of the predicted amino acid sequences from four full-length plant FAAHs (*Arabidopsis*, *M. truncatula*, rice and tomato) and two truncated sequences (grape and wheat) is shown in Fig. 7. Proteins were most divergent at the N-termini and highly conserved within the amidase signature domain (about 150 aa, blue underline). Residues previously determined to be important for NAE hydrolysis by rat FAAH were absolutely conserved in plant sequences (arrows). These conserved residues included K205, S281, S282, S305, and R307 in the *Arabidopsis* FAAH sequence.

A schematic diagram of the domain architecture of plant FAAH proteins is shown in Fig. 8 highlighting the organization of six identifiable domains (panel A). The identified domains were surmised by visual inspection of amino acid sequence alignments of multiple plant FAAH sequences (Fig. 7), and verified by motif elicitation algorithms comparing the three functional plant FAAH proteins, *Arabidopsis*, *M. truncatula* and rice (e.g., MEME and MAST tools at the San Diego State Computing Center; meme.sdsc.edu; [19,20]). Consensus sequences are provided in Fig. 8B, with the amino acids that were identical in six plant FAAH sequences shown in bold capital letters. Any variable amino acid position was denoted with an X, although nearly all substitutions were conservative substitutions with similar amino acids (compare Fig. 7 for specific amino acid substitutions within the consensus sequences). Domain 1 was identified as a variable N-terminus, as this sequence was least similar among plant FAAHs. Domains 2, 3 and 4 spanned the amidase signature sequence, with domains 2 and 4 containing conserved residues important for catalysis in rat FAAH. Domains 5 and 6 showed no homology in domain/motif databases (e.g., cDART, BLOCKS, Pfam, Prosite, etc.), but were regions that were conserved among all plant FAAH members (including predicted peptides from truncated nucleotide sequences of various plant species (Table 1). These C-terminal domains also shared some similarity with the

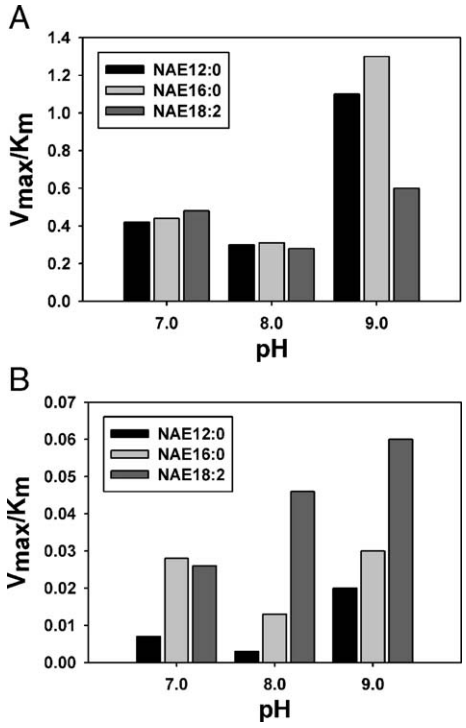

Fig. 4. pH dependence of *A. thaliana* (A) and rice (B) FAAH enzyme activity. Initial velocities were measured at increasing concentrations of respective [1-^{14}C]NAE at each pH (buffered with 50 mM Bis–Tris buffer pH 7.0, 8.0, or 9.0 in a final volume of 0.4 mL). Reactions were initiated by the addition of *E. coli* cell lysates expressing *A. thaliana* or rice FAAH (2 μg for *A. thaliana*, 20 μg for rice). V_{max} and K_m values were calculated from saturation plots as in Fig. 3., and enzyme behavior toward each substrate was plotted vs. reaction pH.

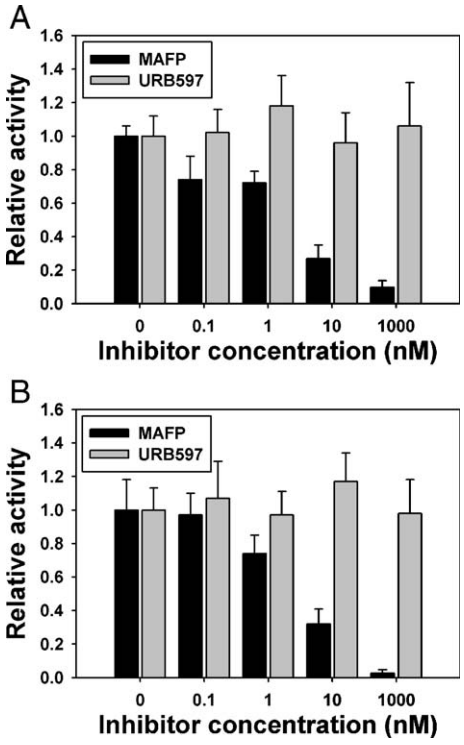

Fig. 5. Effects of MAFP and URB597 on the hydrolysis of [1-^{14}C]NAE18:2 by *A. thaliana* and rice NAE amidohydrolases. Assays were conducted with *E. coli* cell lysates expressing *Arabidopsis* (A) or rice (B) NAE amidohydrolases (2 μg for *A. thaliana*, 20 μg for rice). Reactions were incubated for 30 min at 30 °C with 100 μM [1-^{14}C]NAE18:2 in the absence (0 nM) or presence of increasing concentrations of MAFP or URB597. The data are means ± S.D. of triplicate assays.

C-terminus of mammalian FAAHs [9], although the similarity was not as robust.

3. Discussion

The occurrence of NAEs in biological systems is widespread and includes animals [21], plants [9], and microorganisms [22,23]. Much recent research in mammalian physiology has focused on the function of these lipids as signaling molecules since NAEs activate cannabinoid (CB) receptors [5], vanilloid receptors [24] and peroxisome proliferator receptor-alpha (PPAR) transcription factors [25]. Comparatively little information exists for NAE function in plant systems, although recent studies suggest that these lipids interact with membrane bound receptors to effect changes in ion flux and gene expression [10,11], and in other work, NAEs were shown to be potent inhibitors of phospholipase D (PLD) alpha [26], a PLD family member that seems to be unique to higher plants [27]. The recent discovery of NAEs in *Saccharomyces cerevisiae* [22] has prompted speculation that NAEs function as lipid mediators in microorganisms, but direct evidence for such a role has yet to be reported. Key to understanding the functional roles of these lipids in all organisms is to identify the mechanism(s) that regulate their accumulation. NAE levels in animal systems appear to be modulated by their degradation to free fatty acids and ethanolamine by fatty acid amide hydrolase (FAAH), a member of the amidase superfamily [6]. The recent identification of a functional FAAH homologue in *Arabidopsis* suggests that this mechanism might also operate in plants. Here, this concept gains further support by the identification of FAAH homologues in monocots and legumes. The availability of functionally-defined molecular sequences for these FAAH

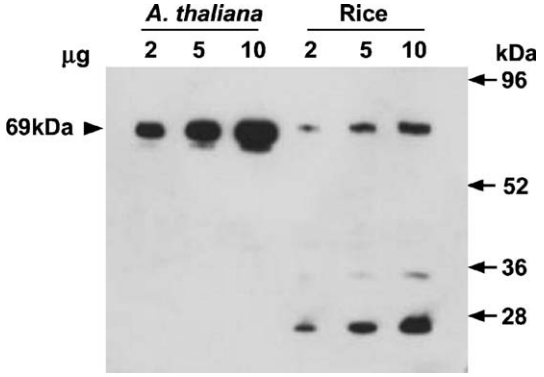

Fig. 6. Western blot analysis of recombinant, epitope-tagged *A. thaliana* and rice FAAH in *E. coli* lysates. Increasing amounts of total *E. coli* lysate (2, 5, or 10 μg protein) expressing *A. thaliana* or rice FAAH were separated by SDS-PAGE and transferred to PVDF membranes. Immobilized proteins were probed with anti-c-*myc* monoclonal antibodies and visualized by indirect chemiluminescence (goat anti-mouse IgG conjugated to horseradish peroxidase). Positions of pre-stained molecular weight standards are indicated on the right, and the predicted molecular weight of the recombinant proteins is marked on the left.

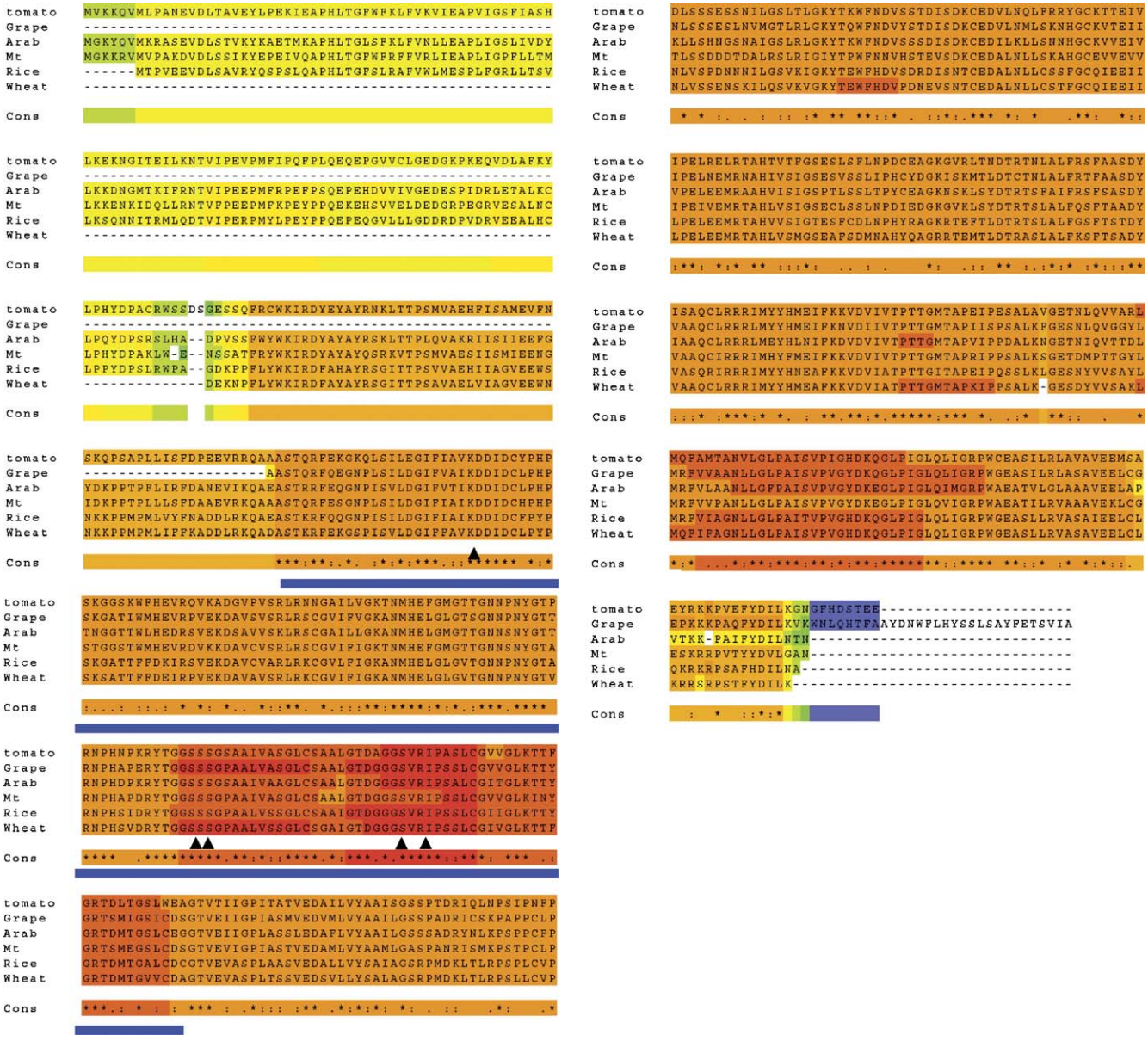

Fig. 7. Alignment of amino acid sequences of plant FAAH proteins including those identified in tomato (TC132131), grape (TC36243), *Arabidopsis* (GenBank accession AY308736; Arab), *Medicago truncatula* (Mt; sequence from Fig. S1), *Oryza sativa* (Rice, sequence from Fig. S2), and wheat. Alignment was generated with T-Coffee algorithms. Wheat and grape sequences are truncated at the N-terminus relative to the other full-length sequences. Colors denote relative similarity with red being highest and blue-green being lowest (yellow-orange is in-between). The consensus sequence (Cons) below all sequences indicates residues that were identical (asterisk) or similar (colon or period) in all sequences. Residues determined to be important for amidase catalysis by the rat FAAH (K205, S281, S282, S305, R307 in the At sequence) are conserved in all plant sequences.

enzymes, coupled with insight into their structural topology, should now facilitate further studies of NAE metabolism in higher plant systems.

To gain insight to structural features of the plant FAAH proteins, we utilized the rat FAAH protein crystal structure ([17]; ExPDB file 1mt5A) as a template for homology-based protein modeling (Fig. 9). Initial comparison of the rat, *Arabidopsis*, rice and *M. truncatula* FAAH protein sequences using BLAST2P2 and SIM algorithms at the Swiss-Model website (http://swissmodel.expasy.org/) identified a region of 153 amino acids in the plant sequences that was of sufficient sequence similarity with rat FAAH for protein modeling (Fig. 9, alignment). This region included domains 2, 3 and 4 (Fig. 8), which spans the core of the amidase signature sequence and possesses the serine–serine–lysine residues of the catalytic triad characterized in other amidases ([17,28]). Visual inspection of the rat FAAH protein (Fig. 9A) demonstrates that domains 2, 3, and 4 are located at predominantly interior regions of the protein structure that collectively form the active site and a portion of the substrate-binding pocket. The plant FAAH sequences were threaded onto corresponding regions of the rat structure to generate energetically favorable structures (energy minimization and Ramachandran plots not shown) that were highly similar to the rat structure, with the exception of a single amino

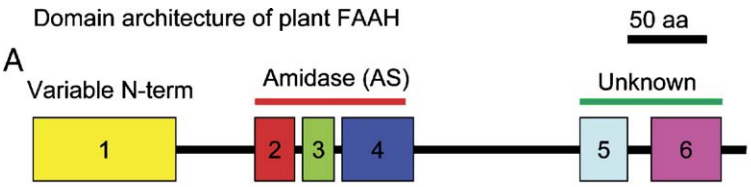

B

Domain	Consensus Sequence	Length (aa)
1	Not applicable (Variable)	100
2	**AST**x**RF**x**G**xxx**S**x**L**x**GIF**xxx**KDDIDC**x**P**x**P**	29
3	**GK**x**NMHE**x**G**x**G**xx**GNN**x**NYGT**x**RNPH**	25
4	**RYTGGSSSG**x**AA**x**V**xx**GLCS**x**A**x**GTD**x**G**x**SVRIP**xx**LCG**xx**GLK**	40
5	**Q**xx**RRR**x**M**x**Y**xxxx**FK**x**VD**x**I**x**TPTTG**x**TAP**x**I**	30
6	**LM**x**F**xxxx**N**x**LG**x**PAI**x**VP**x**G**x**DK**x**GLPIGLQ**xx**GRPW**x**EA**xx**L**	40

Fig. 8. Schematic drawing of the domain architecture of plant FAAH proteins. The putative domains were predicted from available programs and domain databases (InterPro Prosite, ProDom and Pfam) or by regions of high amino acid sequence identity amongst all six FAAH proteins aligned in Fig. 5. A three-part organization to the amidase signature (AS; PF01425) domain is proposed based on the consensus sequence from the six plant proteins. Domain 2 has a conserved lysine (K205 in the *Arabidopsis* sequence) known to be important in catalysis by rat FAAH. Domain 4 has four amino acid residues believed to be important in catalysis (S281, S282, S305, R307 in the *Arabidopsis* sequence). Domains 5 and 6 are of unknown function, but are similar amongst all plant FAAH proteins and these regions share some similarity with mammalian FAAH proteins [9]. The precise consensus sequences are shown. Small x denotes more than one amino acid could occupy that position; however, substitutions were almost always with a similar residue.

acid insertion occurring at a surface-exposed, turn region of the plant structures (Fig. 9B and C). Although the catalytic residues of both plant and rat FAAH proteins are contained exclusively in domains 2 and 4, domain 3 appears to play a critical role in establishing the overall topology of the binding pocket by providing extensive hydrogen bonding interactions with domains 2 and 4 (Fig. 9D). Close inspection of the catalytic domain (Fig. 9E) reveals that all 5 residues previously shown to be essential for enzymatic activity of FAAH proteins are located in the immediate vicinity of the active site pocket. These homology-based models clearly establish the structural relationship of the plant FAAH proteins with FAAHs of vertebrates and will provide a basis for future structure/function studies of this newly identified class of plant enzymes.

Several lines of evidence presented here support the identification of a FAAH family of enzymes in higher plants. First, the genes encoding FAAH proteins from diverse plant species, *Arabidopsis*, rice and *M. truncatula*, appear to have a complex, but highly conserved, structural organization (Fig. 1). Second, cDNAs corresponding to these genes (Figs. S1, S2) were expressed in *E. coli* and these recombinant enzymes indeed possessed FAAH-like biochemical properties (Figs. 2–5). And third, these (and several additional homologous) plant sequences encode proteins with conserved domain architectures (Figs. 7 and 8) and conserved active site domains (Fig. 9). All of the plant sequences were highly similar with 65% identity or better over their entire lengths (Fig. 7; Table 1). These plant sequences were considerably diverged from mammalian FAAH sequences with generally less than 20% identity over their entire lengths [9]. Nonetheless, recombinant proteins from both plants and animal sources expressed in *E. coli* had similar, but not identical, kinetic and biochemical properties, including similar affinities for a broad range of NAEs and potent inhibition by one active-site directed enzyme inhibitor [17] (Figs. 2–5). Taken together these data help to define a new group of enzymes in plants that may have important regulatory functions in terms of modulating the endogenous levels of NAEs.

4. Materials and methods

4.1. Materials

[1-^{14}C]Lauric acid was from Amersham Biosciences. [1-^{14}C]Myristic acid, arachidonic acid, lauric acid, linoleic acid, myristic acid, anandamide, ethanolamine, phenylmethylsulfonyl fluoride (PMSF), and isopropyl β-D-thiogalactopyranoside (IPTG) were from Sigma Chemical Co (St. Louis). [1-^{14}C]Linoleic and [1-^{14}C]palmitic acids were purchased from NEN (Boston, MA). Methyl arachidonyl fluorophosphonate (MAFP) was from TOCRIS (Ellisville, MO), n-dodecyl-β-D-maltoside (DDM) was from Calbiochem (La Jolla, CA), URB597 was from Cayman Chemical (Ann Arbor, MI) and silica gel G (60 Å)-coated glass plates for thin-layer chromatography (10 cm × 20 cm or 20 cm × 20 cm, 0.25 mm thickness) were from Whatman (Clifton, NJ). Specific types of *N*-[1-^{14}C] acylethanolamines (and non-radiolabeled NAEs) were synthesized from ethanolamine and the respective [1-^{14}C]fatty acids (and non-radiolabeled FFAs) by first producing the fatty acid chloride [29] and purified by TLC as described elsewhere [14].

4.2. Bioinformatics and homology modeling

BLAST searches (http://blast.wustl.edu) in *Medicago truncatula* and *Oryza sativa* genome databases were done using the *Arabidopsis thaliana* FAAH gene, At5g64440, as the query sequence. Candidate orthologous FAAH cDNA sequences were identified in gene indices of different plant species curated by the Institute for Genomic Research (TIGR) and available at www.tigr.org. Exon–intron annotation of genes, nucleotide sequence analyses, and protein domain identification were performed using various Internet-based informatics tools and database comparisons including BLAST and cDART (www.ncbi.nlm.nih.gov), ProDom [30], Prosite [31],TMHMM transmembrane and topology predictor [32,33], pSORT [34], BLOCKS (http://blocks.fhcrc.org), MEME (http://meme.sdsc.edu/meme/website/meme.html), ExPASy (http://us.expasy.org/), CLUSTALW [35] and T-Coffee [36]. Some sequence assembly, characterization and alignments were made with DNASIS software (Hitachi). Homology-based modeling was performed using the Swiss-Model interface

```
                          Domain 2 (red)                                  Domain 3 (green)
Rat          119 TDCETQLSQAPRQGLLYGVPVSLKECFSYKGHDSTLGLSL-NEGMPSESDCVVVQVLKLQGAVPFVHTNVPQSMLSF 194
Arabidopsis  182 EASTRRFEQGNPISVLDGIFVTIKDDIDCLPHPTNGGTTWLHEDRSVEKDSAVVSKLRSCGAILLGKANMHELGMGT 258
Medicago     181 AASTQRFESGNPLSILDGIFIAIKDDIDCHPHPSTGGSTWMHEVRDVKKDAVCVSRLRSCGVIFIGKTNMHEFGMGT 257
Rice         176 EASTKRFQQGNPISILDGIFIAIKDDIDCFPYPSKGATTFFDKIRSVEKDAVCVARLRKCGVLFIGKANMHELGLGV 252
                   .  ::...   .:* *: :::*: :.   : :. . :: .:    :.*.. *  *:  *.: : ::*: :  :.

                                  Domain 4 (blue)
Rat          195 DCSNPLFGQTMNPWKSSKSPGGSSGGEGALIGSGGSPLGLGTDIGGSIRFPSAFCGICGLKPTGNRLSKSGLKGCV 270
Arabidopsis  259 TGNNSNYGTTRNPHDPKRYTGGSSSGSAAIVAAGLCSAALGTDGGGSVRIPSALCGITGLKTTYGRTDMTGSLCEG 334
Medicago     258 TGNNSNYGTARNPHAPDRYTGGSSSGPAAIVASGLCSAALGTDGGSSVRIPSSLCGVVGLKINYGRTSMEGSLCDS 333
Rice         253 TGNNPNYGTARNPHSIDRYTGGSSSGPAALVSSGLCSAAIGTDGGGSVRIPSSLCGIIGLKTTYGRTDMTGALCDC 328
                   .*. :* : **   .: .****.* .*::.:* .. .:*** *.*:*:**::**: *** . .* .  *
```

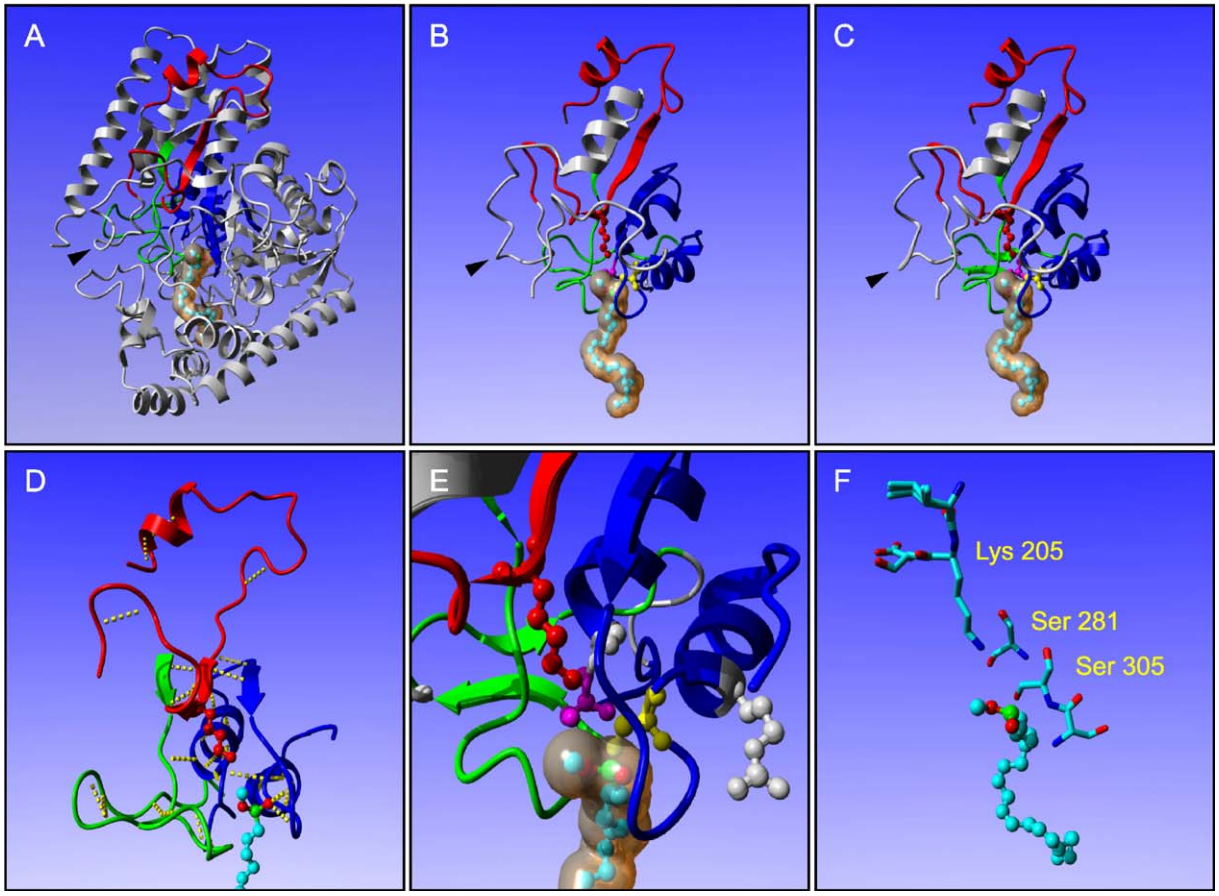

Fig. 9. Structural modeling of plant FAAH proteins. BLAST and SIM alignments performed at the Swiss-Model interface identified a region of 153 amino acids in the plant FAAH proteins that was sufficiently similar to the rat FAAH protein for homology-based modeling. An alignment of these sequences, which includes domains 2, 3, and 4 of the amidase signature, is shown at the top. Each domain is labeled according to the color used to highlight the domains in panels below. Five conserved residues that were previously shown to be essential for FAAH activity (McKinney and Cravatt [6]) are labeled with gray boxes, and the active site residues are in bold. A solid arrowhead indicates the position of a single amino acid insertion in the plant sequences. (A) Structure of the rat FAAH protein (ExPDB file 1mt5A) showing the relative positions of domains 2 (red), 3 (green), and 4 (blue) with the MAFP inhibitor (highlighted with van der Waals radii) co-crystallized in the active site. Solid arrowhead indicates the position of the single amino acid insertion in the plant FAAH sequences, which occurs at a surface-exposed, turn region of the protein structure. (B) Extracted portion of the rat FAAH structure showing the region used for homology-based modeling of the plant proteins. The catalytic triad residues (K142, S217, and S241) are colored red, pink, and yellow, respectively. (C) Overlay of all modeled plant FAAH domains, with MAFP inhibitor docked in the active site. Corresponding active site residues are also colored red, pink, and yellow, respectively. (D) Hydrogen bonding interactions between domains 2, 3, and 4 of the rat protein structure. Note the extensive hydrogen bonding between the β-strands of domains 2, 3, and 4 in the immediate vicinity of the active site (K142 is shown for orientation purposes). (E) Close-up of the overlay for plant FAAH proteins showing the relative positioning of active site residues, including two additional residues (corresponding to S282 and R307 of *Arabidopsis*, both colored grey) that are perfectly conserved among the plant and rat sequences. (F) Overlay of catalytic residues in the plant FAAH active sites showing nearly direct superposition of each side chain. Side chains of all plant FAAH models are shown, and amino acid positions are numbered according to the *Arabidopsis* sequence.

(http://swissmodel.expasy.org/) [37] and the rat FAAH A chain as a template (ExPDB file 1mt5A) [17]. All structures were evaluated and compared using the Swiss-PdbViewer program DeepView, version 3.7 (http://www.expasy.org/spdbv/) [38]. Plant structures were subjected to a final round of energy minimization using the GROMOS96 implementation of DeepView, with harmonic constraints on all α-carbons to restrict movements of the protein

backbone. Parameters included 50 steps of steepest descents followed by 500 steps of conjugate gradients minimization. Final images were composed using YASARA version 5.7.22 (http://www.yasara.org/) and rendered using POV-Ray version 3.6 (http://www.povray.org/).

4.3. cDNA isolation

For *Medicago truncatula* FAAH cDNA isolation, an EST sequence (GenBank accession AW695697) was identified and the corresponding clone was retrieved from the Samuel Roberts Noble Foundation EST collection, and sequenced completely on both strands (2× each, commercial service). The complete nucleotide sequence was deposited in GenBank (DQ091761). For the rice cDNA, sequence-specific primers were designed to the 5′ and 3′ ends of the ORF from the rice gene sequence (Accession number AL606442), and were used for reverse transcriptase (RT)-PCR (forward, 5′-ATGACGCCGGTG-GAGGAGGTGG-3′ and reverse, 5′-AGCGTTCAGGATGTCATGAAATGC-3′). The template for RT-PCR was total RNA extracted from 2-day-old rice seedlings using Trizol reagent (Invitrogen). Fresh seedlings (approx. 400 mg) were harvested, ground to a fine powder in liquid nitrogen, and combined with 2 mL of Trizol reagent for RNA isolation according to the manufacturer's instructions. For RT-PCR, the first-strand cDNA synthesis from total RNA was carried out at 50 °C for 30 min and incubated for 4 min at 94 °C to inactivate the reverse transcriptase. The targeted amplification of the candidate rice FAAH mRNA by Platinum Taq (RT-PCR mixture; Invitrogen) was achieved through 25 cycles of 94 °C for 1 min, 45 °C for 1 min, 72 °C for 2 min followed by a final polymerization step at 72 °C for 7 min. The RT-PCR products were gel-purified and ligated into pTrcHis2 for nucleotide sequencing and protein expression (below). Commercial DNA sequencing of both strands (complete 2× each strand) verified the identity of the cDNA as the rice gene product, and the complete cDNA sequence was deposited in GenBank (DQ118178).

4.4. Protein expression

For *M. truncatula* FAAH protein expression, oligonucleotide primers (forward, 5′-ATGGGGAAGAAGCGTGTAATGG-3′ and reverse, 5′-GTTAGCCCCCAGAACATCGTAG-3′) were designed to amplify only the open reading frame (ORF) of the *M. truncatula* cDNA, and PCR conditions were as above, except that a 10-to-1 ratio of polymerases (Taq-to-Pfu; Invitrogen) was used for amplification and the template was the *M. truncatula* cDNA (GenBank accession DQ091761) in pBluescript SK-. The ORF-PCR products were gel-purified as above, subcloned into pTrcHis2 expression vector, and the constructs introduced into chemically-competent *E. coli* TOP10 cells as host. Transformed colonies were selected with correct in-frame fusions and accurate nucleotide sequence for both *M. truncatula* and rice were determined by sequencing plasmid DNA over the vector insert junctions and by sequencing the inserts completely on both strands.

Selected transformed cell lines were grown in LB medium to an OD_{600} of 0.6 to 0.7 and induced with 1 mM IPTG for 4 h. Pelleted cells were resuspended in lysis buffer (50 mM Tris–HCl, pH 8.0, 100 mM NaCl and 0.2 mM dodecylmaltoside) at a ratio of 1-to-10^8 (*E. coli* cells-to-DDM molecules; 0.1 $OD_{600}=10^8$ cells/mL, Elbing and Brent, 2002). After incubation on ice for 30 min resuspended cells were sonicated on ice with six 10-s bursts at high intensity with a 10-s cooling (ice bath) period between each burst. The selection of DDM as the detergent, and determination of optimal DDM concentration and content ratio was based on empirical comparisons for recovery of solubilized active *Arabidopsis* FAAH enzyme with the highest specific activity [15]. The crude lysates were centrifuged at 105,000×*g* for 1 h in a Sorvall Discovery 90 model ultracentrifuge (Beckman Ti45 rotor) and the supernatants were used for NAE amidohydrolase assays.

4.5. NAE amidohydrolase assays

NAE synthesis and enzyme assays were conducted as previously described [14,15] with a few modifications. The enzyme source was solubilized in 0.2 mM dodecylmaltoside (DDM) and incubated with 100 μM [^{14}C]NAE (20,000 dpm) in 50 mM Bis–Tris buffer (pH 9.0) in 0.2 mM DDM for 30 min to survey for NAE amidohydrolase activity [14,15]. Assays of lysates of *E. coli* cells expressing rat FAAH (WT-FAAH; [16]) or *Arabidopsis* FAAH [15] served as a comparison of NAE amidohydrolase activity, whereas non-transformed cell lysates or cell lysates with the cDNA cloned in reverse orientation with respect to the *lac*Z promoter served as negative controls for activity assays. Initial velocity measurements were made at increasing concentrations of [^{14}C]-labeled NAE species, and reactions were initiated by adding the recombinant enzyme source (2 μg *E. coli* lysate for *Arabidopsis* and 20 μg *E. coli* lysate for rice). Enzyme reactions were terminated by the addition of boiling isopropanol (70 °C) and lipids were extracted into chloroform. Lipid products were separated by TLC and the distribution of radioactivity was evaluated by radiometric scanning [14]. Activity was calculated based on the radiospecific activity of [^{14}C]-labeled substrate. Two irreversible active-site-directed FAAH inhibitors, MAFP and URB597, were used to test the sensitivity of the plant recombinant NAE amidohydrolase activity. Inhibitors were added from a stock solution dissolved in DMSO, and activity was adjusted for minimal solvent effects where necessary based on assays in the presence of the appropriate amount of solvent alone. Protein content was determined by Coomassie blue-dye binding using bovine serum albumin as the protein standard [39].

4.6. Western blotting

Proteins in *E. coli* cell lysates were separated by SDS-PAGE (10% resolving gels) and were electrophoretically transferred to polyvinylidene fluoride (PVDF) membranes (0.2 μm, Bio-Rad, Hercules, CA) in a Semidry Trans-Blot apparatus (Bio-Rad, Hercules, CA) for 40 min at constant 14 V. PVDF membranes were blocked in 5% nonfat milk (Bio-Rad), and recombinant proteins, expressed as c-Myc-epitope fusions, were localized with a 1-to-2000 dilution of mouse monoclonal anti-c-Myc antibodies (ABGENT, San Diego, CA). Immunolocalized proteins were detected by chemiluminescence following incubation with a 1-to-2500 dilution of goat anti-mouse IgG conjugated to horseradish peroxidase (Bio-Rad) according to manufacturer's instructions.

Acknowledgements

The authors thank Dr. Rebecca Dickstein, University of North Texas, for assistance with annotation of the *M. truncatula* FAAH gene, and Dr. Charlene Case, UNT-Center for Plant Lipid Research, for assistance with preparation of the manuscript.

Supported in part by the USDA-CSREES NRI Competitive Grants Program in Plant Biochemistry 2002-35318-12571, the DOE Energy Biosciences Program DE-FG02-05ER15647, and the United States Department of Agriculture (Current Research Information System project number 6435-41000-087-00D).

Appendix A. Supplementary data

Supplementary data associated with this article can be found, in the online version, at doi:10.1016/j.bbalip.2006.03.004.

References

[1] R.I. Wilson, R.A. Nicoll, Endocannabinoid signaling in the brain, Science 296 (2002) 678–682.
[2] B.C. Paria, H. Wang, S.K. Dey, Endocannabinoid signaling in synchronizing embryo development and uterine receptivity for implantation, Chemistry and Physics of Lipids 121 (2002) 201–210.
[3] E.V. Berdyshev, Cannabinoid receptors and the regulation of immune response, Chemistry and Physics of Lipids 108 (2000) 169–190.
[4] L. De Petrocellis, D. Melck, T. Bisogno, V. Di Marzo, Endocannabinoids and fatty acid amides in cancer, inflammation and related disorders, Chemistry and Physics of Lipids 108 (2000) 191–209.

[5] V. Di Marzo, L. De Petrocellis, F. Fezza, A. Ligresti, T. Bisogno, Anandamide receptors, Prostaglandins, Leukotrienes and Essential Fatty Acids 66 (2002) 377–391.
[6] M.K. McKinney, B.F. Cravatt, Structure and function of fatty acid amide hydrolase, Annual Review of Biochemistry 74 (2005) 411–432.
[7] B.F. Cravatt, K. Demarest, M.P. Patricelli, M.H. Bracey, D.K. Giang, B.R. Martin, A.H. Lichtman, Supersensitivity to anandamide and enhanced endogenous cannabinoid signaling in mice lacking fatty acid amide hydrolase, Proceedings of the National Academy of Sciences of the United States of America 98 (2001) 9371–9376.
[8] B.F. Cravatt, A.H. Lichtman, The enzymatic inactivation of the fatty acid amide class of signaling lipids, Chemistry and Physics of Lipids 121 (2002) 135–148.
[9] K.D. Chapman, Occurrence, metabolism, and prospective functions of N-acylethanolamines in plants, Progress in Lipid Research 43 (2004) 302–327.
[10] S. Tripathy, B.J. Venables, K.D. Chapman, N-Acylethanolamines in signal transduction of elicitor perception. Attenuation of alkalinization response and activation of defense gene expression, Plant Physiology (Rockville) 121 (1999) 1299–1308.
[11] S. Tripathy, K. Kleppinger-Sparace, R.A. Dixon, K.D. Chapman, N-acylethanolamine signaling in tobacco is mediated by a membrane-associated, high-affinity binding protein, Plant Physiology (Rockville) 131 (2003) 1781–1791.
[12] E.B. Blancaflor, G. Hou, K.D. Chapman, Elevated levels of N-lauroylethanolamine, an endogenous constituent of desiccated seeds, disrupt normal root development in *Arabidopsis thaliana* seedlings, Planta 217 (2003) 206–217.
[13] K.D. Chapman, B. Venables, R. Markovic, R.W. Blair Jr., C. Bettinger, N-Acylethanolamines in seeds. Quantification of molecular species and their degradation upon imbibition, Plant Physiology (Rockville) 120 (1999) 1157–1164.
[14] R. Shrestha, M.A. Noordermeer, M. van der Stelt, G.A. Veldink, K.D. Chapman, N-acylethanolamines are metabolized by lipoxygenase and amidohydrolase in competing pathways during cottonseed imbibition, Plant Physiology (Rockville) 130 (2002) 391–401.
[15] R. Shrestha, R.A. Dixon, K.D. Chapman, Molecular identification of a functional homologue of the mammalian fatty acid amide hydrolase in *Arabidopsis thaliana*, Journal of Biological Chemistry 278 (2003) 34990–34997.
[16] M.P. Patricelli, H.A. Lashuel, D.K. Giang, J.W. Kelly, B.F. Cravatt, Comparative characterization of a wild type and transmembrane domain-deleted fatty acid amide hydrolase: identification of the transmembrane domain as a site for oligomerization, Biochemistry 37 (1998) 15177–15187.
[17] M.H. Bracey, M.A. Hanson, K.R. Masuda, R.C. Stevens, B.F. Cravatt, Structural adaptations in a membrane enzyme that terminates endocannabinoid signaling, Science 298 (2002) 1793–1796.
[18] J.P. Alexander, B.F. Cravatt, Mechanism of carbamate inactivation of FAAH: implications for the design of covalent inhibitors and in vivo functional probes for enzymes, Chemistry & Biology 12 (2005) 1179–1187.
[19] T.L. Bailey, M. Gribskov, Methods and statistics for combining motif match scores, Journal of Computational Biology 5 (1998) 211–221.
[20] T.L. Bailey, M. Gribskov, Combining evidence using *P* values: application to sequence homology searches, Bioinformatics 14 (1998) 48–54.
[21] H.H. Schmid, E.V. Berdyshev, Cannabinoid receptor-inactive N-acylethanolamines and other fatty acid amides: metabolism and function, Prostaglandins, Leukotrienes and Essential Fatty Acids 66 (2002) 363–376.
[22] O. Merkel, P.C. Schmid, F. Paltauf, H.H. Schmid, Presence and potential signaling function of N-acylethanolamines and their phospholipid precursors in the yeast *Saccharomyces cerevisiae*, Biochimica et Biophysica Acta 1734 (2005) 215–219.
[23] H.H. Schmid, P.C. Schmid, V. Natarajan, N-acylated Glycerophospholipids and their Derivatives, Progress in Lipid Research 29 (1990) 1–43.
[24] V. Di Marzo, P.M. Blumberg, A. Szallasi, Endovanilloid signaling in pain, Current Opinion in Neurobiology 12 (2002) 372–379.
[25] J. LoVerme, G. La Rana, R. Russo, A. Calignano, D. Piomelli, The search for the palmitoylethanolamide receptor, Life Sciences 77 (2005) 1685–1698.
[26] S.L. Austin-Brown, K.D. Chapman, Inhibition of phospholipase D alpha by N-acylethanolamines, Plant Physiology (Rockville) 129 (2002) 1892–1898.
[27] X. Wang, Multiple forms of phospholipase D in plants: the gene family, catalytic and regulatory properties, and cellular functions, Progress in Lipid Research 39 (2001) 109–149.
[28] S. Shin, T.H. Lee, H.M. Koo, S.Y. Kim, H.S. Lee, Y.S. Kim, B.H. Oh, Crystallization and preliminary X-ray crystallographic analysis of malonamidase E2, an amidase signature family member, Acta Crystallographica. Section D, Biological Crystallography 58 (2002) 562–563.
[29] C.J. Hillard, W.S. Edgemond, W.B. Campbell, Characterization of ligand binding to the cannabinoid receptor of rat brain membranes using a novel method: application to anandamide, Journal of Neurochemistry 64 (1995) 677–683.
[30] F. Servant, C. Bru, S. Carrere, E. Courcelle, J. Gouzy, D. Peyruc, D. Kahn, ProDom: automated clustering of homologous domains, Briefings in Bioinformatics 3 (2002) 246–251.
[31] C.J. Sigrist, L. Cerutti, N. Hulo, A. Gattiker, L. Falquet, M. Pagni, A. Bairoch, P. Bucher, PROSITE: a documented database using patterns and profiles as motif descriptors, Briefings in Bioinformatics 3 (2002) 265–274.
[32] A. Krogh, B. Larsson, G. von Heijne, E.L. Sonnhammer, Predicting transmembrane protein topology with a hidden Markov model: application to complete genomes, Journal of Molecular Biology 305 (2001) 567–580.
[33] E.L. Sonnhammer, G. von Heijne, A. Krogh, A hidden Markov model for predicting transmembrane helices in protein sequences, Proceedings (International Conference on Intelligent Systems for Molecular Biology) 6 (1998) 175–182.
[34] K. Nakai, M. Kanehisa, A knowledge base for predicting protein localization sites in eukaryotic cells, Genomics 14 (1992) 897–911.
[35] J.D. Thompson, D.G. Higgins, T.J. Gibson, CLUSTAL W: improving the sensitivity of progressive multiple sequence alignment through sequence weighting, position-specific gap penalties and weight matrix choice, Nucleic Acids Research 22 (1994) 4673–4680.
[36] C. Notredame, D.G. Higgins, J. Heringa, T-Coffee: a novel method for fast and accurate multiple sequence alignment, Journal of Molecular Biology 302 (2000) 205–217.
[37] T. Schwede, J. Kopp, N. Guex, M.C. Peitsch, SWISS-MODEL: An automated protein homology-modeling server, Nucleic Acids Research 31 (2003) 3381–3385.
[38] N. Guex, M.C. Peitsch, SWISS-MODEL and the Swiss-PdbViewer: an environment for comparative protein modeling, Electrophoresis 18 (1997) 2714–2723.
[39] M.M. Bradford, A rapid and sensitive method for the quantitation of microgram quantities of protein utilizing the principle of protein-dye binding, Analytical Biochemistry 72 (1976) 248–254.